All solid-state electrochemical capacitors using N,N-dimethylpyrrolidinium fluorohydrogenate as ionic plastic crystal electrolyte

AUTHOR(S):

Taniki, Ryosuke; Matsumoto, Kazuhiko; Nohira, Toshiyuki; Hagiwara, Rika

CITATION:

Taniki, Ryosuke ...[et al]. All solid-state electrochemical capacitors using N,N-dimethylpyrrolidinium fluorohydrogenate as ionic plastic crystal electrolyte. Journal of Power Sources 2014, 245: 758-763

ISSUE DATE:

2014-01

URL:

http://hdl.handle.net/2433/178039

All solid-state electrochemical capacitors using *N,N*-dimethylpyrrolidinium fluorohydrogenate as ionic plastic crystal electrolyte

Ryosuke Taniki, Kazuhiko Matsumoto*, Toshiyuki Nohira, Rika Hagiwara

Graduate School of Energy Science, Kyoto University, Sakyo-ku, Kyoto 606-8501, Japan,

*E-mail: k-matsumoto@energy.kyoto-u.ac.jp

Tel: +81-75-753-5822

Fax: +81-75-753-5906

Abstract

An electrochemical capacitor using an ionic plastic crystal of *N*,*N*-dimethypyrrolidinium fluorohydrogenate (DMPyr$(FH)_2F$) as a solid electrolyte has been successfully operated with activated carbon electrodes at 298 K. Typical square-shapes for electric double-layer capacitors are observed in the cyclic voltammogram within the narrow potential regions. In the wide potential regions, the redox reactions involving fluorohydrogenate anions occur on both the positive and negative electrodes. The galvanostatic charge–discharge test confirms stable operation of the electrochemical capacitor using the present ionic plastic crystal. The capacitances of the positive and negative electrodes are 263 and 221 F g^{-1} (capacitance per gram of electrode weight), respectively, at the 300^{th} cycle when the cell is charged up to the voltage of 2.5 V with a current density of 238 mA g^{-1}. The ac impedance test shows that ions in the ionic plastic crystal form double-layer between electrolyte and internal surface of the pore of activated carbon. The open-circuit voltage decreases proportionally to the square root of time within the first 10 s after galvanostatic charging, which confirms that the ions in the ionic plastic crystal inhomogeneously distributed in the pore of activated carbon migrate to be homogeneous under a diffusion-limited process.

Key words: electrochemical capacitor; ionic plastic crystal; fluorohydrogenate salt; activated carbon; double-layer; redox capacitor

1. Introduction

Electric double-layer capacitors store electric energy by formation of double-layer between an electronic conductive electrode and an ionic conductive electrolyte. Their non-Faradaic charge–discharge mechanism generally offers high power density and long cycle life. Performance of capacitors is evaluated by the power density of IV and energy density of $1/2CV^2$, where C, I, and V denote the capacitance, current density, and operation voltage which has a strong correlation with ionic conductivity and electrochemical stability of electrolytes [1–4]. Another type of electrochemical capacitor, pseudocapacitor, is also widely studied. Charge storage of pseudocapacitor is based on reversible electrochemical reactions on redox active electrodes such as metal oxides (RuO_2, Fe_3O_4, and MnO_2) [5–7] and electrically conductive polymers (polyaniline and polythiophene) [8,9]. These materials exhibit fast charge transfer reactions and high diffusivity of redox active species in electrodes.

Replacement of liquid electrolytes to solid electrolytes for electrochemical capacitors offers prevention of electrolyte leakage, flexible and thin configuration of devices, volumetric stability during the cell operation, and easy packing and handling [10–12]. Gel polymer electrolytes have been widely studied as solid electrolytes because they have preferable features as solid electrolytes for electrochemical capacitors [10–13]. Gel polymer electrolytes are formed by mixing the polymer host, solvent, and salt, where the polymer host acts simply as a stiffener for the low molecular weight solvent working as a medium for the mobility of cationic and anionic species [14]. Ionic conductivities of gel polymer electrolytes utilizing aqueous solvents, organic solvents, and ionic liquids (ILs) for electrochemical capacitors range between 10^0 – 10^1 mS cm^{-1}, 10^{-1} – 10^0 mS cm^{-1}, and 10^{-1} – 10^0 mS cm^{-1}, respectively [10,12,13,15–17]. These values are lower than those of liquid electrolytes by an order of magnitude.

Ionic plastic crystals (IPCs), which entirely consist of ions and show negligible vapor

pressure, non-flammability, and good thermal and electrochemical stability, are studied as a new class of solid electrolytes for electrochemical devices such as batteries, fuel cells, and dye-sensitized solar cells [18–23]. Ionic plastic crystal is a mesophase formed between an ionic crystal and IL and characterized by a long-range positional order and rotating motions of component ions [24,25]. Entropy of fusion is usually quite small for IPCs, reflecting the rotational modes of the component ions. The rotational behavior contributes to the formation of defects, which gives a liquid-like feature such as a fast ion diffusion in either matrix or doped materials and gives plastic mechanical properties [26,27]. While organic salts based on nonaromatic onium cations, such as pyrrolidinium, tetraalkylammonium, tetraalkylphosphonium, and trialkylsulfonium cations, often form room temperature ILs, those with short alkyl chains sometimes exhibit IPC phases around room temperature [18–27]. So far, there is no report on utilization of IPCs as solid electrolytes in electrochemical capacitors. Although some IPCs have ionic conductivities of 10^{-1} – 10^{0} mS cm^{-1} (e.g., *N*-ethyl-*N*-methylpyrrolidinium bis(trifluoromethanesulfonyl)amide (EMPyrTFSA) with a small amount of LiTFSA dopant and *N*,*N*-diethyl-*N*-methyl-*N*-(*n*-propyl)ammonium trifluoromethyltrifluoroborate ($N_{1223}CF_3BF_3$) with a small amount of $LiCF_3BF_3$ dopant) [18,20,28], further improvement in ionic conductivity is required for electrochemical capacitors to lower internal resistance and enable operation at a high current density.

Our recent studies showed that IPCs based on fluorohydrogenate anions exhibit high ionic conductivities, (e.g., 5 mS cm^{-1} at 323 K for tetraethylphosphonium fluorohydrogenate and 10.3 mS cm^{-1} at 298 K for *N*,*N*-dimethylpyrroridinium fluorohydrogenate ($DMPyr(FH)_2F$)) [29,30]. These values are comparable to those of typical ionic liquid electrolytes and interesting candidates as solid state electrolytes. It is worth mentioning that electrochemical capacitors using activated carbon electrodes and fluorohydrogenate IL electrolytes have larger capacitances and voltage dependence of capacitance than those of

conventional ILs and organic electrolytes [31–34]. This behavior results from two different Faradaic reactions at the positive and negative activated carbon electrodes contribute to the redox capacitances [34]. The present study reports the first all solid-state electrochemical capacitors using an neat IPC electrolyte. The above-mentioned highly conductive fluorohydrogenate IPC, $DMPyr(FH)_2F$, was used as solid electrolyte in combination with activated carbon electrodes.

2. Experimental

2.1 Electrolytes and electrode materials

The electrolytes, $DMPyr(FH)_2F$ and $EMPyr(FH)_{2.3}F$, were synthesized by the reaction of the starting chloride (DMPyrCl (Yoyu Lab.) and EMPyrCl (Yoyu Lab.)) and anhydrous HF (Daikin Industries, Co. Ltd., >99%), as reported in the literature [30,35]. The 1-ethyl-3-methylimidazolium tetrafluoroborate ($EMImBF_4$, Kanto Kagaku) IL was dried at 393 K prior to use. Activated carbon sheet electrodes with 0.5 mm thickness, composed of 85 wt% of activated carbon made from phenol resin (surface area: 2000 $m^2\ g^{-1}$, mean pore diameter: 2.14 nm, and total pore volume: 1.10 $cm^3\ g^{-1}$), 10 wt% of PTFE, and 5 wt% of carbon black, were dried under vacuum at 453 K overnight. For the charge–discharge test, ac impedance test, and self-discharge test, the sheet electrodes were cut into discs (weight: 21.0 mg and diameter: ~10 mm) both for positive and negative electrodes. The sheet electrodes were cut into discs (weight: 5.0 mg and diameter: ~5 mm) for cyclic voltammetry. Although $DMPyr(FH)_2F$ IPC can be formed into a self-supporting disc (Fig. S1, Suppelementary contents), it was once melted and impregnated into the activated carbon electrode under vacuum above its melting point (325 K) in the present study for better contact with the electrodes. Then, it was cooled down to room temperature where it forms IPC. Impregnation of the other IL electrolytes was performed under vacuum at room temperature.

2.2 Electrochemical measurements

Electrochemical measurements were performed at 298 K under an Ar atmosphere with the aid of a VSP electrochemical measurement system (Bio-Logic). A three-electrode test cell was assembled with a pair of activated carbon sheet electrodes, vitreous carbon current collectors, PTFE separators, and a Ag foil quasi-reference electrode. The Ag foil was inserted between two separators and the potentials of the positive and negative electrodes were separately monitored during electrochemical measurements. Before starting electrochemical measurements, the potentials of the electrodes were monitored overnight to confirm their steadiness.

The galvanostatic charge–discharge tests were performed in the three-electrode cell for 300 cycles at different current densities of 238, 476, and 2380 mA g^{-1}, where the cell was charged up to a voltage of 2.5 V. The charging voltages were controlled based on the voltage between the positive and negative electrodes. Cyclic voltammetry was carried out in the three-electrode cell at a scan rate of 0.2 mV s^{-1}. The ac impedance tests were performed in the two-electrode cell (without Ag quasi-reference electrode) at the applied ac amplitude of 10 mV within the frequency range of 10 kHz to 2 mHz. The self-discharge tests were performed by monitoring the cell voltage for 24 h after constant current charging up to 1.0 V at 238 mA g^{-1} or constant voltage charging at 1.0 V for 1 hour in the two-electrode cell. Two ILs, $EMPyr(FH)_{2.3}F$ and $EMImBF_4$, were used as electrolytes to compare the results of the impedance tests and self-discharge tests.

3. Results and discussion

3.1 Double-layer formations and redox reactions on activated carbon electrodes in fluorohydrogenate IPC

Fig. 1 shows cyclic voltammograms of the activated carbon electrode in DMPyr(FH)$_2$F IPC for the negative potential region between –1.6 and +0.5 V vs. Ag QRE. In the potential region above –0.5 V, a square shape corresponding to the formation of the electric double-layer is observed. In this region, more $DMPyr^+$ cations are present on the surface of the activated carbon electrode than $(FH)_nF^-$ anions are. As shown in the previous study for DMPyr(FH)$_{2.0}$F IPC, only $(FH)_nF^-$ works as a charge carrier in the IPC phase and the long-range migration of $DMPyr^+$ cations does not occur [30]. A conceivable explanation about the double-layer formation in this potential region is that $(FH)_nF^-$ around the surface of the activated carbon electrode migrates away from the electrode and $DMPyr^+$ in the vicinity of the electrode comes close to the surface by exchanging itself with anions. A cathodic current due to a Faradaic reaction is observed below –0.5 V vs. Ag QRE. In correspondence to this, an increase in anodic current is observed in the following anodic scan (coulombic efficiency of 97% when the reverse potential is –1.6 V vs. Ag QRE). In this potential range, electrochemical behavior of the activated carbon electrode in DMPyr(FH)$_2$F IPC is similar to that of EMPyr(FH)$_{2.3}$F IL, and the redox reaction in DMPyr(FH)$_2$F IPC is considered to involve the reduction of $(FH)_nF^-$ and adsorption of atomic hydrogen to the activated carbon [34].

Fig. 2 shows cyclic voltammograms of the activated carbon electrode in DMPyr(FH)$_2$F IPC for the positive potential region between 0 and +1.9 V vs. Ag QRE. When the potential sweep is reversed at +0.5 V vs. Ag QRE, a square shape corresponding to the formation of the double-layer is observed. Because of the large diffusion coefficient of the anion in the IPC phase of DMPyr(FH)$_2$F (3.44×10^{-7} cm^2 s^{-1} at 298 K) [30], the $(FH)_nF^-$ diffuses to the electrode and is adsorbed on the electrode during the anodic scan. An anodic current due to a Faradaic reaction is observed above +0.7 V vs. Ag QRE. The corresponding cathodic current is observed in the following cathodic scan (coulombic efficiency of 93% when the reverse

potential is 1.1 V vs. Ag QRE). As in the case of electrochemical capacitors utilizing EMPyr$(FH)_{2.3}F$ IL, this redox reaction in the positive potential range is the oxidation of carbon accompanied by absorption of $(FH)_nF^-$ or F^- into the activated carbon [34].

3.2 Galvanostatic charge–discharge characteristics

Fig. 3 shows charge and discharge capacitances of the electrochemical capacitors utilizing DMPyr$(FH)_2F$ IPC during the 300 galvanostatic charge–discharge cycles up to the voltage of 2.5 V with a current density of 238 mA g^{-1}. Stable operation of this electrochemical capacitor was confirmed during this test. During the initial three cycles, the charge capacitances for both the positive and negative electrodes are considerably higher than the discharge capacitances due to the irreversible redox reactions between anions and activated carbon. The respective coulombic efficiencies at the 1st, 2nd, and 3rd cycles are 65.7, 86.6, and 90.7% for the positive electrode, and 83.4, 91.8, and 94.5% for the negative electrode. They are, however, improved to 99.1 and 98.9% at the 20th cycle for the positive and negative electrodes, respectively. After the 20th cycle, the coulombic efficiencies exceed 99% for both the electrodes, and the capacitances of the positive and negative electrodes at the 300th cycle are 263 and 221 F g^{-1}, respectively. It is worth mentioning that electrochemical capacitors using EMPyr$(FH)_{2.3}F$ IL showed the capacitances of 290 and 246 F g^{-1} at the positive and negative electrodes at the 300th cycle, respectively [26]. Although the replacement of the electrolytes from fluorohydrogenate IL to fluorohydrogenate IPC slightly decreases the capacitance, the values obtained for fluorohydrogenate IPC are still quite large compared to the case of the typical IL EMImBF$_4$ (168 F g^{-1}, single-electrode capacitance calculated from the cell capacitance in ref. 32).

Fig. 4 shows the charge–discharge curves of the cell, and activated carbon positive and negative electrodes in DMPyr$(FH)_2F$ IPC at the 1st, 10th, and 300th cycles. The potentials of

the positive and negative electrodes reach +1.0 and –1.5 V vs. Ag QRE, respectively, during the charge–discharge tests when the cell is charged to 2.5 V. As shown in Figs. 1 and 2, both the Faradaic reactions occur in these potential ranges. The redox reactions in addition to the double-layer capacitances contribute to the large capacitances obtained in the galvanostatic charge–discharge test.

Fig. 5 shows the capacitances obtained during the 300 galvanostatic charge–discharge cycles to 2.5 V at different current densities of 238, 476, and 2380 mA g^{-1}. The different behavior of the positive and negative capacitances during the first 10 cycles is presumably due to the irreversible electrochemical reactions, penetration of electrolytes, and activation of carbon on the activated carbon electrode. The respective capacitances at large current densities of 476 and 2380 mA g^{-1} at the 300th cycle were 215 and 115 F g^{-1} for the positive capacitance, and 199 and 79 F g^{-1} for the negative capacitance, respectively. Since both the redox reactions do not follow the high rate charge–discharge, the capacitances decrease with increase in the charge–discharge rate.

3.3 The electrolyte resistance in the pore of activated carbon electrode

By means of an ac impedance analysis, the electrolyte resistance is separated into the resistance of the bulk electrolyte (R_{bulk}) and the resistance of the electrolyte from the top to the bottom of the pores (R_{pore}) in the activated carbon. A transmission model of the porous electrode gives a typical behavior of double-layer capacitors characterized by the Nyquist plot in which a slope with a phase angle of –45° (eq. 1) in the high frequency range and a locus in parallel with the imaginary axis (eq. 2) in the low frequency range appear [36,37].

$$Z = R_{bulk} + (R_{pore} / 2\,\omega C_{dl})^{1/2}\,(1 - j) \quad (1)$$

$$Z = R_{bulk} + R_{pore} / 3 - j / \omega C_{dl} \quad (2)$$

where Z, ω, C_{dl}, and j denote impedance, angular frequency, double-layer capacitance, and

imaginary unit, respectively. Figs. 6 (a) and (b) show Nyquist plots of impedance spectra for electrochemical capacitors utilizing DMPyr(FH)$_2$F IPC, EMPyr(FH)$_{2.3}$F IL, and EMImBF$_4$ IL, of which conductivities at room temperature are 10.3, 74.6, and 13 mS cm^{-1}, respectively [3,30,35]. The shape of Nyquist plot for electrochemical capacitors using DMPyr(FH)$_2$F IPC confirms the formation of double-layer between the DMPyr(FH)$_2$F IPC and the activated carbon forming the pore as in the cases for EMPyr(FH)$_{2.3}$F and EMImBF$_4$. The values of R_{bulk} and R_{pore} have been determined to be 2.4 and 26.6 Ω for DMPyr(FH)$_2$F, 1.3 and 6.6 Ω for EMPyr(FH)$_{2.3}$F, and 2.5 and 31.4 Ω for EMImBF$_4$. The R_{pore} values roughly reflect the ionic conductivities of the electrolytes. The R_{bulk} values do not show a relation with the ionic conductivities of the electrolytes because the R_{bulk} value contains the contribution from other factors such as contact resistance and the difference in distance between the two electrodes.

3.4 Migration of ions in the pore of activated carbon electrode

The diffusion behavior of ions composing DMPyr(FH)$_2$F IPC in the pore of activated carbon was investigated by monitoring the open-circuit voltage (V_{oc}) after galvanostatic charging. When an activated carbon electrode is galvanostatically charged, the gradient of the applied potential along the depth direction in the pore gives an inhomogeneous distribution of charge, depending on the depth in the pore. While the activated carbon at the top edge of the pore is charged sufficiently, the one at the bottom in the pore is not. Just after the galvanostatic charging, an open-circuit voltage decreases by homogenization of the charge distribution in the pore (i.e., the diffusion of ions in the pore). In the diffusion-limited process of ions during the homogenization, the open-circuit voltage decreases proportionally to the square root of time ($t^{1/2}$) [38]. Figs. 7 (a), (d), and (g) show time dependence of V_{oc} in electrochemical capacitors using DMPyr(FH)$_2$F IPC, EMPyr(FH)$_{2.3}$F IL, and EMImBF$_4$ IL, respectively, after charging up to 1 V at a current density of 238 mA g^{-1}. The respective IR drops of the cell due to the bulk electrolyte

resistance are 11, 6, and 9 mV, respectively. Figs. 7 (b), (e), and (h) show the relation between V_{oc} and $t^{1/2}$, and Figs. 7 (c), (f), and (i) are the magnifications of (b), (e), and (h) in the range of $t^{1/2} < 10$. The linear decrease in V_{oc} against $t^{1/2}$ during the early 10 seconds is observed for DMPyr(FH)$_2$F IPC in Fig. 7 (c), indicating the migration of ions in the pore certainly occurs in the IPC phase as in the case for EMImBF$_4$ IL (Fig. 7 (i)). The linear decrease in V_{oc} against $t^{1/2}$ in this time region is not clearly observed for EMPyr(FH)$_{2.3}$F due to its low R_{pore}. When the electrochemical capacitors are charged by a constant voltage mode, the migration of ions in the pore is not observed for any electrolyte as seen in Fig. S2 (Supplementary contents).

4. Conclusion

The behavior of the activated carbon electrode in DMPyr(FH)$_2$F IPC was investigated by charge–discharge tests, cyclic voltammetry, and ac impedance spectroscopy. In cyclic voltammetry, the square shapes corresponding to the formation of electric double-layer were observed for both positive and negative activated carbon electrodes in a narrow potential range. The formation of electric double-layer was also confirmed by impedance spectroscopy based on the transmission model. The redox reactions on both the electrodes occur in a wide potential range as reported for EMPyr(FH)$_{2.3}$F IL. Stable operation of the electrochemical capacitor using DMPyr(FH)$_2$F IPC was confirmed for 300 cycles and the capacitances of the positive and negative electrodes at the 300th cycle were 263 and 221 F g^{-1}, respectively. Just after galvanostatic charging, the ions in DMPyr(FH)$_2$F IPC inhomogeneously distributed in the pore of activated carbon, then they migrate to be homogeneous under a diffusion-limited process.

Acknowledgements

The authors would like to thank The Hattori Hokokai Foundation for their financial support to

this work.

Appendix A. Supplementary data

Supplementary data associated with this article can be found, in the online version, at doi:xxxxxx.

References

[1] P. Simon, Y. Gogotsi, Nat. Mater. 7 (2008) 845–854.

[2] E. Frackowiak, F. Béguin, Carbon 39 (2001) 937–950.

[3] A. B. McEwen, H. L. Ngo, K. LeCompte, J. L. Goldman, J. Electrochem. Soc. 146 (1999) 1687–1695.

[4] E. Frackowiak, Phys. Chem. Chem. Phys. 9 (2007) 1774–1785.

[5] C.-C. Hu, W.-C. Chen, K.-H. Chang, J. Electrochem. Soc. 151 (2004) A281–A290.

[6] N.-L. Wu, S.-Y. Wang, C.-Y. Han, D.-S. Wu, L.-R. Shiue, J. Power Sources 113 (2003) 173–178.

[7] T. Brousse, M. Toupin, R. Dugas, L. Athouël, O. Crosnier, D. Bélanger, J. Electrochem. Soc. 153 (2006) A2171–A2180.

[8] K. Zhang, L. L. Zhang, X. S. Zhao, J. Wu, Chem. Mater. 22 (2010) 1392–1401.

[9] M. Mastragostino, C. Arbizzani, F. Soavi, Solid State Ionics 148 (2002) 493–498.

[10] N. A. Choudhury, S. Sampath, A. K. Shukla, Energy Environ. Sci. 2 (2009) 55–67.

[11] K. Naoi, M. Morita, Electrochem. Soc. Interface Spring (2008) 44–48.

[12] A. Lewandowski, A. Świderska, Solid State Ionics 161 (2003) 243–249.

[13] Y. Matsuda, K. Inoue, H. Takeuchi, Y. Okuhama, Solid State Ionics 113–115 (1998) 103–107.

[14] C. A. Vincent, Prog. Solid State Chem. 17 (1987) 145–261.

[15] N. A. Choudhury, A. K. Shukla, S. Sampath, S. Pitchumani, J. Electrochem. Soc. 153 (2006) A614–A620.

[16] T. Osaka, X. Liu, M. Nojima, T. Momma, J. Electrochem. Soc. 146 (1999) 1724–1729.

[17] A. Lewandowski, A. Świderska, Appl. Phys. A 82 (2006) 579–584.

[18] Z. Zhou, H. Matsumoto, Electrochem. Commun. 9 (2007) 1017–1022.

[19] H.-B. Han, J. Nie, K. Liu, W.-K. Li, W.-F. Feng, M. Armand, H. Matsumoto, Z.-B. Zhou,

Electrochim. Acta. 55 (2010) 1221–1226.

[20] D. R. MacFarlane, J. Huang, M. Forsyth, Nature 402 (1999) 792–794.

[21] L. Jin, K. M. Nairn, C. M. Forsyth, A. J. Seeber, D. R. MacFarlane, P. C. Howlett, M. Forsyth, J. M. Pringle, J. Am. Chem. Soc. 134 (2012) 9688–9697.

[22] U. A. Rana, M. Forsyth, D. R. MacFarlane, J. M. Pringle, Eletrochim. Acta 84 (2012) 213–222.

[23] Q. Li, X. Chen, J. Zhao, L. Qiu, Y. Zhang, B. Sun, F. Yan, J. Mater. Chem, 22 (2012) 6674–6679.

[24] J. M. Pringle, P. C. Howlett, D. R. MacFarlane, M. Forsyth, J. Mater. Chem 20 (2010) 2056–2062.

[25] J. M. Pringle, Phys. Chem. Chem. Phys. 15 (2013) 1339–1351.

[26] D. R. MacFarlane, P. Meakin, J. Sun, N. Amini, M. Forsyth, J. Phys. Chem. B 103 (1999) 4164–4170.

[27] D. R. MacFarlane, M. Forsyth, Adv. Mater. 13 (2001) 957–966.

[28] M. Forsyth, J. Huang, D. R. MacFarlane, J. Mater. Chem. 10 (2000) 2259–2265.

[29] T. Enomoto, S. Kanematsu, K. Tsunashima, K. Matsumoto, R. Hagiwara, Phys. Chem. Chem. Phys. 13 (2011) 12536–12544.

[30] R. Taniki, K. Matsumoto, R. Hagiwara, K. Hachiya, T. Morinaga, T. Sato, J. Phys. Chem. B 117 (2013) 955–960.

[31] M. Ue, M. Takeda, A. Toriumi, A. Kominato, R. Hagiwara, Y. Ito, J. Electrochem. Soc. 150 (2003) A499–A502.

[32] A. Senda, K. Matsumoto, T. Nohira, R. Hagiwara, J. Power Sources 195 (2010) 4414–4417.

[33] K. Matsumoto, K. Takahashi, A. Senda, T. Nohira, R. Hagiwara, ECS Trans. 33 (2010) 421–427.

[34] R. Taniki, K. Matsumoto, T. Nohira, R. Hagiwara, J. Electrochem. Soc. 160 (2013) A734–

A738.

[35] K. Matsumoto, R. Hagiwara, Y. Ito, Electrochem. Solid-State Lett. 7 (2004) E41–E44.

[36] R. D. Levie, Electrochim. Acta 8 (1963) 751–780.

[37] M. Itagaki, S. Suzuki, I. Shitanda, K. Watanabe, H. Nakazawa, J. Power Sources 164 (2007) 415–424.

[38] B. E. Conway, Electrochemical Supercapacitors: Scientific Fundamentals and Technological Applications, Kluwer Academic/Plenum, New York, 1999, pp. 557–596.

Figure captions

Fig. 1 Cyclic voltammograms of an activated carbon electrode in DMPyr(FH)$_2$F IPC at 298 K. Scan range: –1.6 and +0.5 V vs. Ag QRE. WE: activated carbon. Scan rate: 0.2 mV s^{-1}.

Fig. 2 Cyclic voltammograms of an activated carbon electrode in DMPyr(FH)$_2$F IPC at 298 K. Scan range: 0 and +1.9 V vs. Ag QRE. WE: activated carbon. Scan rate: 0.2 mV s^{-1}.

Fig. 3 (a) Charge and (b) discharge capacitances of the activated carbon positive (○) and negative (●) electrodes in DMPyr(FH)$_2$F IPC during 300 charge–discharge cycles at a current density of 238 mA g^{-1} at 298 K.

Fig. 4 Charge–discharge curves of the capacitor cell and activated carbon positive and negative electrodes in DMPyr(FH)$_2$F IPC at the 1st, 10th, and 300th cycles at a current density of 238 mA g^{-1} at 298 K.

Fig. 5 Discharge capacitances of the activated carbon (a) positive and (b) negative electrodes in DMPyr(FH)$_2$F IPC (○: 238 mA g^{-1}, □: 476 mA g^{-1}, and ◇: 2380 mA g^{-1}) at 298 K.

Fig. 6 Nyquist plots of the impedance spectra for electrochemical capacitors using (♦) DMPyr(FH)$_2$F IPC, (■) EMPyr(FH)$_{2.3}$F IL, and (●) EMImBF$_4$ IL at the rest potential at 298 K, where (b) is the magnification of (a). The frequency ranges from 10 kHz to 2 mHz.

Fig. 7 Plots of V_{oc}-t and V_{oc}-$t^{1/2}$ after galvanostatic charging for electrochemical capacitors utilizing DMPyr(FH)$_2$F IPC [(a), (b), and (c)], EMPyr(FH)$_{2.3}$F IL [(d), (e), and (f)], and EMImBF$_4$ IL [(g), (h), and (i)], respectively, where (c), (f), and (i) are the magnifications of

dotted parts in (b), (e), and (h).

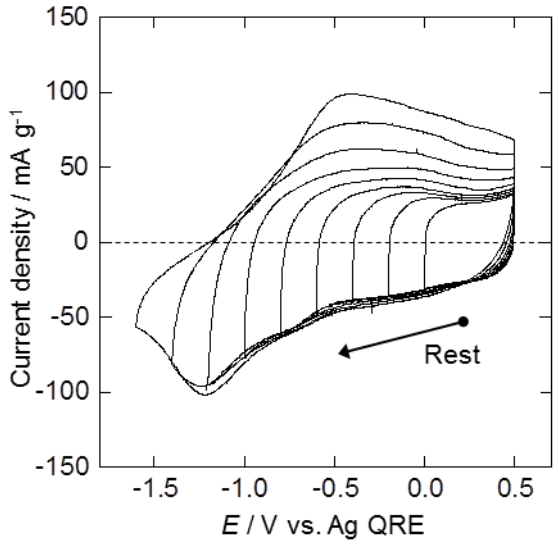

Fig. 1

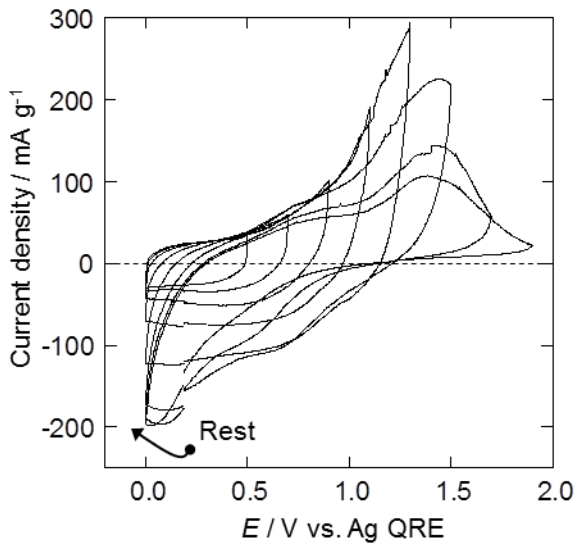

Fig. 2

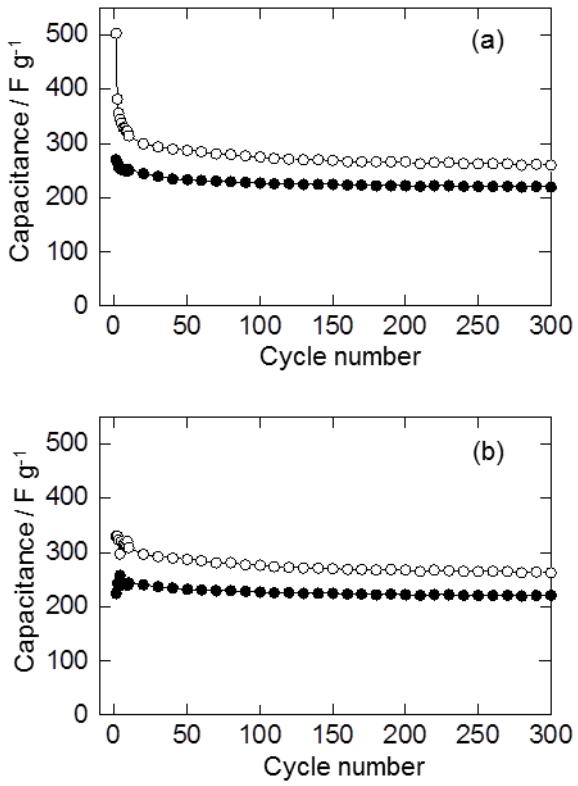

Fig. 3

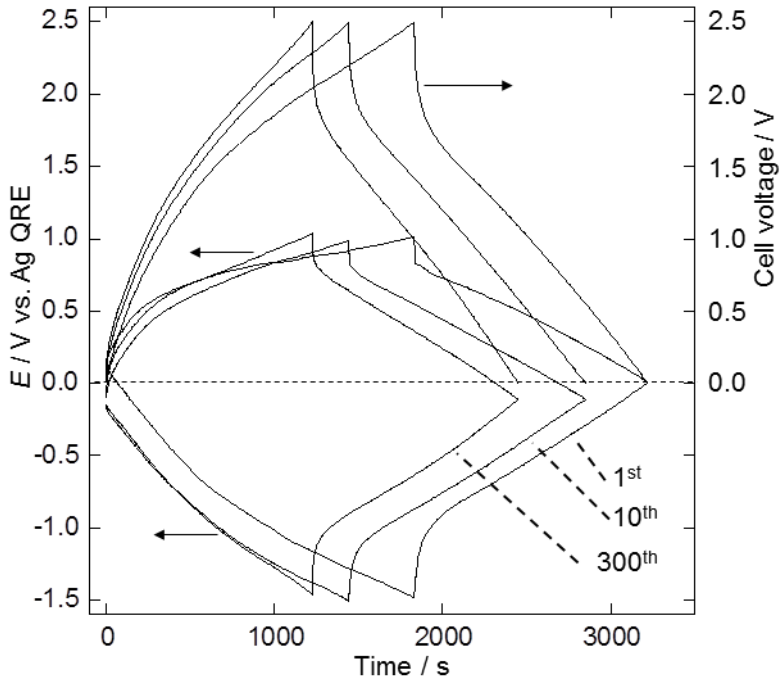

Fig. 4

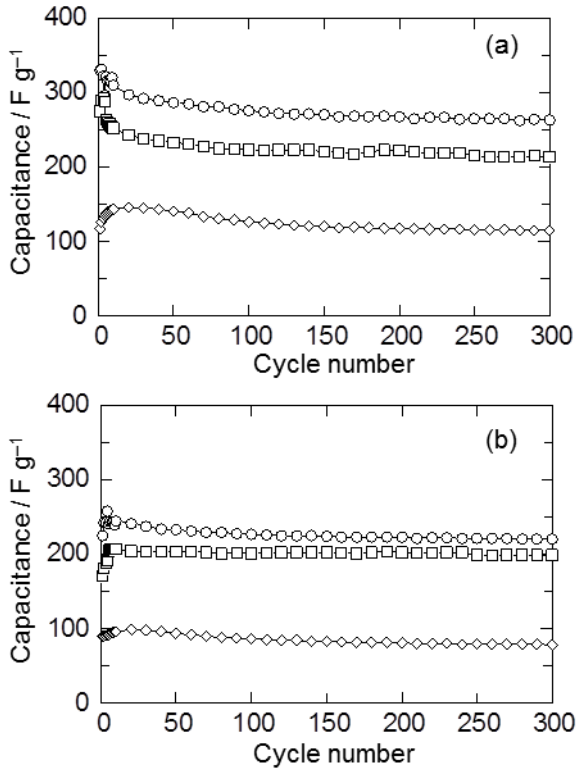

Fig. 5

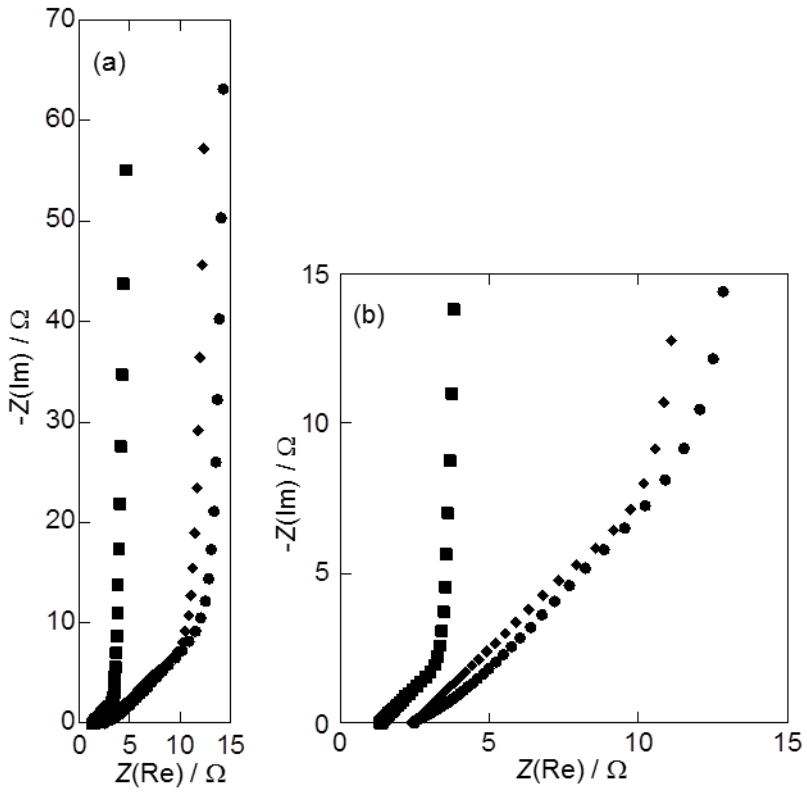

Fig. 6

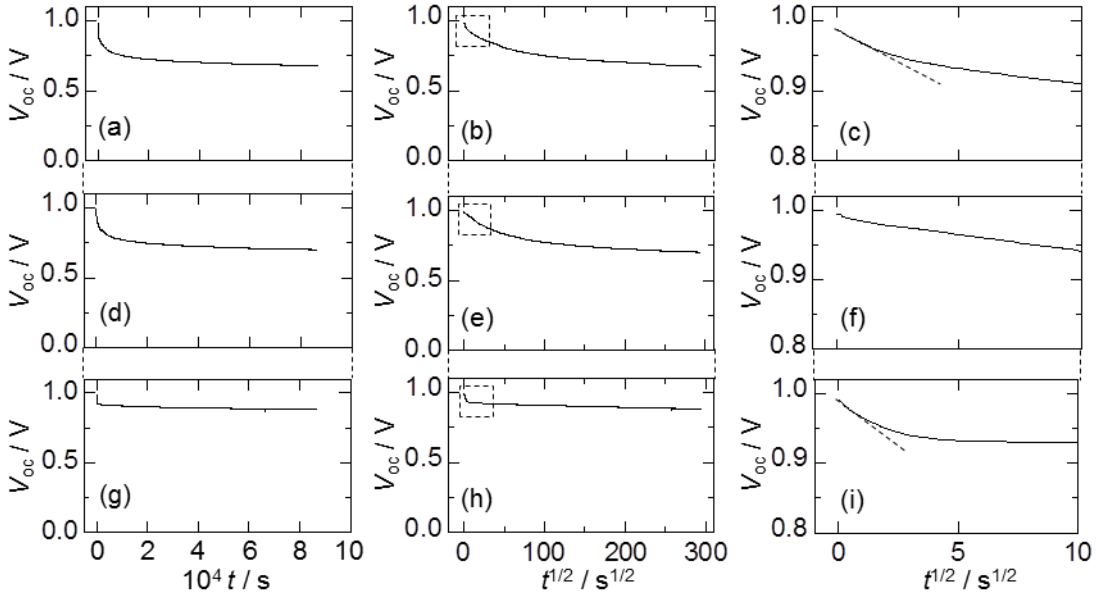

Fig. 7